JOURNAL OF SOLID STATE CHEMISTRY **41**, 293–307 (1982)

Notes on Phases Occurring in the Binary Tungsten–Oxygen System

J. BOOTH,*,† T. EKSTRÖM,‡ E. IGUCHI,*,§ AND R. J. D. TILLEY*

**School of Materials Science, University of Bradford, West Yorkshire BD7 1DP, United Kingdom, and ‡Department of Inorganic Chemistry, Arrhenius Laboratory, University of Stockholm, S-106 91 Stockholm, Sweden*

Received August 24, 1981; in revised form October 26, 1981

The phases occurring in the binary tungsten–oxygen system in the composition region WO_3–WO_2 have been clarified by electron microscopy and powder X-ray diffraction in the temperature range from 723 to 1373 K. There are five structure types in the binary system, besides WO_3, viz., the {102} *CS* structures, the {103} *CS* structures, $W_{24}O_{68}$, $W_{18}O_{49}$, and WO_2. The {102} and {103} *CS* structures, and $W_{24}O_{68}$ structures, were always disordered and true equilibrium was not achieved even after 5 months of heating at 1373 K. The lowest temperature for the formation of the *CS* phases was of the order of 873 K, and the disordered $W_{24}O_{68}$ structure formed at somewhat higher temperatures. The formation of the latter phase was also slower than the formation of the *CS* phases. The results suggest that elastic strain energy is of importance in controlling the microstructures found in the nonstoichiometric regions.

Introduction

The tungsten–oxygen system is of some importance technologically in view of the use of tungsten metal and its compounds in a variety of applications and because the metal is invariably prepared by reduction from oxide precursors at elevated temperatures. Because of this there have been a number of attempts to determine the phases present in the binary tungsten–oxygen system and the conditions under which they are stable. In addition, the reduction path and the crystal habit and size of intermediate phases are of some interest, as in technological processes, such as the preparation of tungsten powders from WO_3; these variables can have a significant effect upon the quality of the final product.

Establishing the phase relations has not been easy and early studies were often contradictory. The first work to substantially clarify the situation was by Magnéli and coworkers, who identified and determined the crystal structures of the lower oxides $W_{20}O_{58}$ (*1*), $W_{18}O_{49}$ (*2*), and WO_2 (*3*), as well as the fully oxidized parent WO_3. These studies, which involved the use of careful and precise powder X-ray diffraction as well as single-crystal techniques, were unable to throw much more light on the system because of the high degree of disorder found in most of the phases prepared by conventional techniques, although it was suggested that a few other oxides related to $W_{20}O_{58}$ also existed (*4*, *5*). These early results have been summarized on a phase diagram published by St. Pierre *et al.* (*6*) and extended by Phillips and Chang (*7*, *8*).

---

† Permanent address: ICI Corporate Laboratory, The Heath, Runcorn, Cheshire, United Kingdom.

§ Permanent address: Department of Metallurgical Engineering, Yokohama National University, Tokiwadai, Hodogaya-ku, Yokohama, 240 Japan.

0022-4596/82/030293-15$02.00/0

More recently the structures occurring when WO_3 is reduced have been clarified considerably by using transmission electron microscopy. Thus Tilley (*9*), Allpress *et al.* (*10*), and Ijima (*11*) have studied very slightly reduced crystals of WO_3 and found them to contain disordered crystallographic shear (*CS*) planes lying on {102} planes. Sundberg and Tilley (*12*) studied crystals which were somewhat more reduced and which covered the range of compositions between WO_3 and about $WO_{2.90}$ and observed both {102} and {103} *CS* planes. Allpress and Gadó (*13*), who made the first electron microscope study of the tungsten oxides, observed disorder in oxides of overall composition near to $WO_{2.90}$, and Sundberg (*14, 15*) has characterized oxides of composition $W_{24}O_{70}$ and $W_{25}O_{73}$ which occur in this phase region. Pickering and Tilley (*16*) reported on the structures occurring in the region between $WO_{2.90}$ and $W_{2.72}$, and reported the existence of an oxide phase of composition close to $WO_{2.82}$ which may be identical to that reported earlier by Glemser *et al.* (*17*). The structure of this material, $W_{24}O_{68}$, has recently been determined using electron microscopy by Sundberg (*18*), who showed that it consists essentially of a WO_3-like matrix containing pentagonal column (*PC*) elements. More recently Berglund and Sahle (*19*) have studied the phases formed when carefully controlled oxygen pressures are used and Sahle and Sundberg (*20*) have reported the occurrence of disordered *PC* elements in *CS* phases prepared under these controlled conditions. Further information on the phases occurring in the binary tungsten–oxygen system and their relationships with some phases in the ternary tungsten oxides is given in the articles by Tilley (*21*) and Ekström and Tilley (*22*). Finally, we can note that Sarin (*23*) has made a study of the morphology of the crystals formed during the hydrogen reduction of WO_3.

These studies allow a reasonable picture to be drawn of the structures occurring when WO_3 is reduced. Many of them are, though, fragmented and do not allow an accurate assessment of the phase ranges of the various structure types to be determined, especially as heating times of hours or days have been used, which are usually too short to achieve equilibrium. This has meant that it has not been possible to compare the theoretical considerations of phase stability with precise phase analytical data, although the study of Berglund and Sahle (*19*) at 1270 K was made under controlled conditions and is therefore of some importance in this respect. Nevertheless, there is still a need for information from a wider range of temperatures. In this paper we have attempted to summarize the typical phases formed in sealed-tube experiments over the temperature range between 723 and 1373 K. We have paid particular attention to the low-temperature region and the phases present after extended heating times of up to 5 months. These data have not been presented before and go some way in clarifying the nature of the complex series of nonstoichiometric phases that exist near to WO_3 in the binary tungsten–oxygen system.

Experimental

Samples with overall compositions in the range WO_2 to WO_3 were prepared from tungsten metal turnings and WO_3 powder of "Specpure" quality supplied by Johnson Matthey Ltd. Appropriate weights of reactants were sealed into silica ampoules and heated for periods of time varying from several days to 5 months at temperatures in the range 723–1373 K. The ampoules were usually evacuated, but sometimes they were filled with about $\frac{1}{3}$ atm of HCl to act as a mineralizing and transporting agent.

After reaction, samples were examined optically and, where possible, crystals of differing habit or appearance were separated manually. Most samples were studied by high-resolution electron microscopy. For this, crystals were crushed under *n*-butanol in an agate mortar. A drop of the resultant suspension was then allowed to dry on a net-like carbon film supported on a copper grid. Crystal fragments which projected over holes in the net were examined using a JEM 100B electron microscope operated at 100 kV and fitted with a goniometer stage. In addition, many samples were studied using X-ray diffraction by recording their powder patterns at room temperature in a Guinier–Hägg focusing camera using Cu$K\alpha_1$ radiation and KCl (a = 0.6292 nm) as an internal standard. The positions of lines on the films were determined visually or by means of an Abrahamsson automatic film scanner. Evaluation of the film data and indexing and refinement of the unit cell parameters were performed by computer, using programs written by Brandt and Nord (*24*). Finally, a few samples were studied by scanning electron microscopy using a JSM 35 microscope.

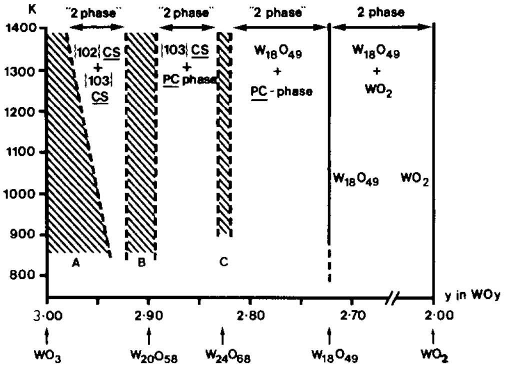

FIG. 1. Schematic representation of the phases occurring in the WO_3–WO_2 region of the binary *W–O* system. Most phase regions have uncertain boundaries and equilibrium is not usually achieved, the structures being disordered. Thus region A contains disordered/quasi-ordered {102} *CS* phases, region B contains more or less well-ordered {103} *CS* phases, and region C contains disordered *PC* phases of the $W_{24}O_{68}$ type. $W_{18}O_{49}$, on the contrary, appears to be a strictly stoichiometric equilibrium phase. The stoichiometry range of WO_2 was not studied.

Results

Six different structure types were found in the preparations studied, viz., WO_3, the {102} *CS* phases, the {103} *CS* phases, $W_{24}O_{68}$, $W_{18}O_{49}$, and WO_2. With the exception of $W_{24}O_{68}$, all of these phases are stable over the temperature range 873–1373 K investigated in this study. This latter phase was not found in our preparations at 873 K, but we have been unable to determine whether this is because the material is unstable at this temperature or merely because of kinetic reasons. In practice the composition range between WO_3 and approximately $WO_{2.80}$ contains a number of very disordered regions, which will be discussed below. The oxide $W_{18}O_{49}$ appeared to be a stoichiometric phase with no measurable composition range. There was no special attempt made to study the composition range over which WO_2 existed, but the present study confirmed that no additional phase occurred in the composition range between $W_{18}O_{49}$ and WO_2 even after very long heating times. The composition ranges over which the various structures occurred is shown schematically in Fig. 1.

Samples Heated at 1373 K for up to 2 Weeks

Apart from $W_{18}O_{49}$ and WO_2, disorder was found to be severe in these preparations. Equilibrium was not readily achieved, and although the structures formed quickly, with little difference being found between the samples heated for 3 days and those heated for 2 weeks, there was no sign of an increase in ordering over this time scale. Invariably after heating each sample was found to have separated into two parts, a vapor-transported fraction and a residue, which was often recrystallized. The ratio of the structure types present in the vapor-transported fraction was always different from that in the residue. We cannot, therefore, talk of the equilibrium situation as this clearly does not occur in 2 weeks of heating, but we can describe the phase makeup of the samples as prepared. The notes below refer to samples heated for 2 weeks and not shorter periods of time.

In samples with overall compositions between WO_3 and $WO_{2.995}$ only {102} *CS* phases were found, but it is possible that very small amounts of {103} *CS* phases are also present but were not detected. Certainly in samples with overall compositions between $WO_{2.995}$ and $WO_{2.925}$ both {102} and {103} *CS* phases were confirmed; the amount of {103} *CS* material increased as the composition fell. The {102} *CS* crystals were usually chunky in habit, resembling WO_3, while the {103} *CS* crystals were needle like, making analysis by optical microscopy relatively straightforward. Mixed crystals containing both {102} and {103} *CS* planes were not found in our preparations at this fairly high temperature.

The microstructures of the crystals containing {102} *CS* planes showed considerable disorder. The *CS* planes occurred on a number of equivalent {102} orientations and existed in isolation, in small groups, or as quasi-ordered arrays. Very occasionally a reasonably large area of crystal contained a fairly well-ordered array of {102} *CS* planes, but these were never so well ordered as to produce a discrete set of superlattice spots on the electron diffraction pattern rather than a continuous streak in the {102} direction. On the basis of *CS* plane density the maximum degree of reduction of these crystals was never below $WO_{2.98}$ even when in contact with {103} *CS* phase crystals, and this must be regarded as the lower limit of the {102} phase range at this temperature. Most crystal fragments, though, had compositions far closer to WO_3, as stated.

Most of these microstructures have been adequately illustrated in other publications (*9–22*) and will not be shown here. There are two features to mention which have not been discussed extensively in the past which are shown in Figs. 2a, b, and c. In Fig. 2a we show a low density of intersecting *CS* planes. In these situations one of the *CS* planes invariably terminated before intersection. The distance at which they terminated is of interest for calculation of *CS* plane interaction energies (*25*) and in the present survey it was found to vary widely; the closest approach being approximately 1.5 nm. The manner in which the *CS* planes terminated also varied, with some *CS*

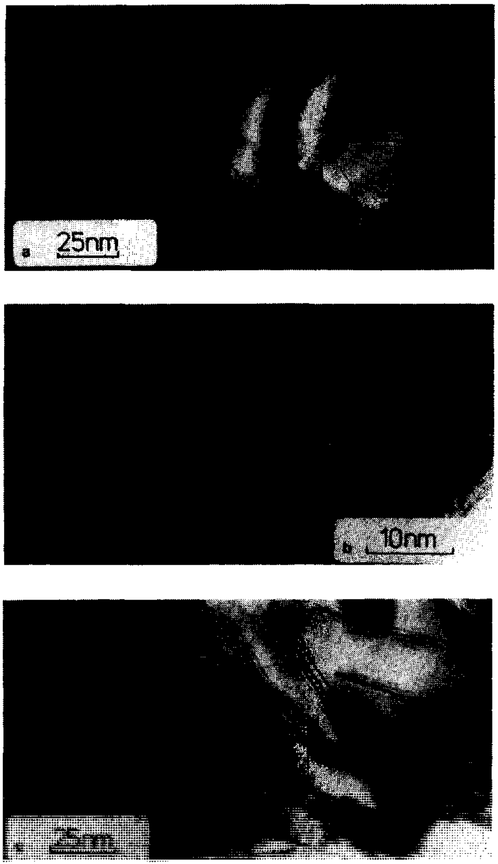

FIG. 2. (a) Low-resolution electron micrograph of intersecting {102} *CS* planes in slightly reduced WO_3. (b) Ill-defined chevrons of darker strain contrast and (c) short *CS* plane segments in slightly reduced WO_3.

planes ending in a dislocation, some in a short row of pentagonal columns of the sort described by Sahle and Sundberg (*20*), and some being deflected into a new orientation.

The other feature of interest is shown in Figs. 2b and c. In crystals showing this type of contrast the diffraction patterns showed no significant amounts of streaking, but the crystal flake often showed a wrinkled appearance with chevrons of darker contrast on {102} clearly visible (Fig. 2b). Higher magnification micrographs showed dark ill-defined chevron-like patterns, which were sometimes, but not always, resolved into short segments of {102} *CS* planes (Fig. 2c). As can be seen from Fig. 2c, the *CS* planes are not uniformly straight and some irregularity is seen to occur. Although the correlation is not absolutely certain a reasonable interpretation of the dark chevron-like regions is that they represent strained regions of crystal, perhaps due to {102} *CS* planes in the course of formation which have not yet penetrated throughout the whole of the crystal thickness. Rather similar features have been reported by Ijima (*11*), but in this case the features were produced by electron beam irradiation.

In slightly reduced WO_3 samples containing a fair number of {102} *CS* planes, powder X-ray diffraction showed that the high-temperature orthorhombic form of WO_3 persisted to room temperature. This behavior has, in fact, been reported previously (*28*) and it was suggested that in the presence of {102} *CS* planes the transformation from the high-temperature orthorhombic form to the monoclinic room-temperature form was hindered or blocked. The transformation involves no radical structural changes, merely a change in the displacements of the WO_6 octahedra in the matrix. This change is not observed in our electron micrographs, but the symmetry shift is readily detected on a powder X-ray photograph. Hence we have found that the occurrence of the high-temperature orthorhombic form of WO_3, together with the room-temperature monoclinic form of WO_3 as recorded by powder X-ray diffraction, is a valuable diagnostic test for the presence of {102} *CS* planes in the WO_3 crystals. This is so even when the *CS* planes are disordered and produce no other X-ray diffraction evidence or patterns.

The {103} *CS* structures occurred alone only in samples with compositions between the limits of $WO_{2.920}$ and $WO_{2.895}$. Above this upper composition, {102} *CS* phases were also found and below the lower composition limit $W_{24}O_{68}$ and sometimes $W_{18}O_{49}$ were found. The {103} *CS* planes were much better ordered than their {102} counterparts. Although streaking occurred in the diffraction patterns a fair number contain sharp spots, and the n value in the series formula W_nO_{3n-2} can be evaluated with a reasonable degree of accuracy. The range found was from a maximum of $n = 25$, i.e., $W_{25}O_{72}$ ($WO_{2.92}$), to $W_{15}O_{43}$ ($WO_{2.87}$). This agrees well with previous estimates of this phase range for samples prepared in a similar way (*16, 19*).

The $W_{24}O_{68}$ phase seemed to occur alone only over a narrow composition range close to $WO_{2.82}$–$WO_{2.83}$. This is not to say, though, that a well-ordered structure formed, and, in most of the preparations made at 1373 K for 2 weeks, they were very disordered and did not yield very satisfactory X-ray films. In fact the X-ray powder patterns showed only the WO_3 subcell reflections with certainty and as such they could not be indexed or differentiated from the X-ray powder patterns of the lower {103} *CS* phases. Electron microscopy confirmed that the crystals were extremely disordered, with the walls of pentagonal column units, which characterize the structure, usually linked together in the same way as in the ordered phase, but with a great deal of twinning present and separated by variable widths of WO_3-like struc-

TABLE I

The X-Ray Powder Pattern of $W_{18}O_{49}$[a]

d_{obsd} (nm)	I_{obsd}	$\|F\|^2_{obsd}$	*hkl*	$\sin^2\theta_{obsd} \times 10^5$	Δ
1.314	122	7	$\bar{1}01$	343	0
1.272	660	43	001	366	−1
0.8476	135	20	101	825	+2
0.8278	154	24	200	865	+2
0.6568	39	10	$\bar{2}02$	1,375	0
0.6104	80	24	$\bar{3}01$	1,592	+1
0.5234	92	39	102	2,165	−1
0.4591	148	84	$\bar{1}03$	2,814	+7
0.4549	122	70	$\bar{4}01$	2,866	+5
0.4437	312	191	$\bar{4}02$	3,013	+8
0.4383	78	48	$\bar{3}03$	3,088	−4
0.3908	12	9	$\bar{4}03$	3,886	0
0.3784	2,507	2,169	010	4,144	+1
0.3737	1,220	1,082	103	4,249	+3
0.3642	1,223	1,146	$\bar{3}02$	4,473	+5
0.3523	12	12	401	4,781	+1
0.3496	44	45	302	4,853	0
0.3407	1,033	1,121	$\bar{5}03$	5,111	+4
0.3396	516	561	$\bar{1}04$	5,144	+2
0.3316	45	51	500	5,396	+1
0.3278	41	48	$\bar{2}12$	5,516	−2
0.3250	149	178	203	5,617	+2
0.3217	33	40	$31\bar{1}$	5,734	0
0.3175	437	552	004	5,883	−1
0.3055	176	241	$\bar{6}02$	6,355	−5
0.3026	126	176	504	6,477	−4
0.2960	340	499	$\bar{6}03$	6,772	+12
0.2943	286	425	402	6,850	+7
0.2919	669	1,014	501	6,961	−1
0.2880	82	128	$\bar{4}12$	7,152	+4
0.2864	22	34	$\bar{3}13$	7,235	−3
0.2805	159	262	$\bar{3}05$	7,539	0
0.2782	76	127	$\bar{2}05$	7,666	+4
0.2764	383	654	600	7,764	−4
0.2749	541	934	$\bar{4}05$	7,848	−2
0.2720	33	58	$\bar{4}13$	8,021	−8
0.2658	904	1,678	113	8,396	+7
0.2625	805	1,622	$\bar{5}12$	8,611	+1
0.2567	32	64	312	9,002	+6
0.2527	971	2,005	$\bar{1}14$	9,287	+2
0.2492	94	200	510	9,555	+17
0.2481	39	84	403	9,639	−4
0.2466	123	268	213	9,755	0
0.2433	213	479	014	10,023	−5
0.2378	131	309	$\bar{6}12$	10,495	−8
0.2365	105	251	105	10,610	0
0.2333	287	706	$\bar{6}13$	10,900	−4
0.2324	192	476	412	10,985	0
0.2312	485	1,217	511	11,099	−6

ture. In crystals which were closer in composition to WO_3, regions of {103} *CS* and of the disordered $W_{24}O_{68}$ structure were sometimes found to coexist, behavior which is quite different than that at the {102}/{103} *CS* boundary at this temperature, suggesting that the $W_{24}O_{68}$ structure may be able to form from the {103} *CS* structure type.

In contrast to this behavior, the oxide $W_{18}O_{49}$ was well ordered. Crystal fragments examined in the electron microscope were only rarely twinned and other disorder has not been observed. This is in good accord with powder X-ray data, as the films show very sharp reflections which usually suggest that the crystals are not appreciably disordered. From a practical point of view the oxide $W_{18}O_{49}$ ($WO_{2.722}$) can be looked upon as a stoichiometric phase with no or a very limited composition range. This is in agreement with the previous findings by Marucco *et al.* (*27*), who reported a very narrow composition range $WO_{2.7196}$–$WO_{2.7224}$, or the X-ray phase analysis by Ekström (*28*). The X-ray films of all $W_{18}O_{49}$ samples were sharp and readily measured with high precision. A typical result is shown in Table 1.

In Table 2 we collected together a few typical electron microscope analyses of some samples within the composition range WO_3–$WO_{2.80}$. This reveals clearly the inhomogeneity of the samples. It should be stressed that these data apply to an ordinary series of preparations, and that other

---

[a] Data were recorded at room temperature using a Guinier–Hägg camera with strictly monochromatic Cu$K\alpha_1$ radiation. The observed integrated intensities I_{obsd} were obtained by film scanner process and the corresponding $|F|^2_{obsd}$ values after correction for polarization. Lorentz and geometric factors were obtained by computer routines. In the table, $\Delta = 10^5 \times (\sin^2\theta_{obsd}$-$\sin^2\theta_{calcd})$. A refinement of the monoclinic cell parameters gave $a = 1.8324 \pm 2$ nm, $b = 0.3784 \pm 1$ nm, $c = 1.4035 \pm 2$ nm, and $\beta = 115.20 \pm 1°$.

TABLE II

A TYPICAL ELECTRON MICROSCOPE ANALYSIS OF SOME BINARY W–O SAMPLES PREPARED BY HEATING FOR 2 WEEKS AT 1373 K REVEALING NONEQUILIBRIUM

Composition O/W	No. of crystals examined	{102} *CS*	Disordered {103}	{103} *CS* (*n*)										"$W_{24}O_{68}$" type
				24	23	22	21	20	19	18	17	16	15	
2.995	11	11												
2.975	12	11		1										
2.980	14	11	2	1										
2.965	14	13	1											
2.950	23	13	2						1	1	1	2		
2.940	14	9	2	1	1		1							
2.925	41	22	1	4		1	4		1	4	1	2	1	
2.910	14	3	4	5		2								
2.900	24	2				4	1		2	10	1	4		
2.895	28	?	4						5	12				?
2.880	23	?	6							9				?
2.865	20	0	2						1	2	1			14
2.857	25	1										2	1	21
2.850	9	0								1				8
2.820	23	0										2		21
2.800	21	0							1			2		18

similar series of preparations will almost certainly have a somewhat different distribution of structures. In particular we can note that the phase $W_{20}O_{58}$, one of the first *CS* structures to be characterized by Magnéli (*1*), was not present in these preparations. Also it is worth recording the fact that no significant differences in phase analysis were found between samples heated in vacuum and those heated in HCl vapor.

The difficulty of using powder X-ray diffraction as a phase analytical tool is also apparent from Table 2. As mentioned above, {102} *CS* phases were only indicated on the X rays by the presence of both the orthorhombic and monoclinic forms of WO_3, an indirect method of analysis only justified by the prior combination of X-ray and electron microscope results. For the {103} *CS* phases the problem is equally severe. The X-ray powder patterns of the {103} *CS* structures were often very diffuse and the only reflections that were reasonably sharp were of the type (*hk*O), as the *a* and *b* axes of the {103} *CS* phases vary but little from one W_nO_{3n-2} homolog to another. The superstructure reflections relating to the different *c* axes were usually weak or absent, and when present formed diffuse or broad bands. Attempts to index such patterns were meaningless. Even in samples heated for much longer periods of time (vide infra), X-ray analysis is still difficult. The $W_{24}O_{68}$ phase posed similar problems as remarked above. In general, therefore, the X-ray analysis was used only as a broad characterizing tool, its main advantage being in the recognition of WO_3 and $W_{18}O_{49}$ in our preparations.

Samples Heated at 1373 K for 5 Months

In order to determine whether the disorder found in samples heated for up to 2 weeks would be changed by prolonged heating, a series of samples were heated for a period of 5 months. The most important feature of note in these samples was that the transported fraction of the product was similar in phase composition to the part which had recrystallized but had not transported. It was found that the {102} component of the *CS* phases was almost identical to that of the samples heated for only 2 weeks at 1373 K. As before, very disordered regions occurred and also quasi-ordered arrays, but the latter were never well enough ordered to give sharp superlattice spots on the electron diffraction patterns.

The {103} phases yielded much sharper diffraction patterns than the corresponding samples heated for shorter times. Even so, there was still a spread of *CS* plane spacings present, revealed by the presence of $W_{18}O_{52}$ in a sample of composition $WO_{2.90}$ and the presence of {102} *CS* fragments in a sample of overall composition $WO_{2.93}$. The maximum range found for the {103} *CS* structures did not vary significantly compared to that observed in the samples heated for shorter times, being from approximately $W_{25}O_{72}$ to $W_{15}O_{43}$. Nevertheless, the increased sharpness of the electron diffraction patterns and the narrower spread of *n* values in these preparations lead to sharper and clearer X-ray powder patterns. However, even in these cases the samples are nowhere near monophasic and

TABLE III

THE X-RAY POWDER PATTERN OF A SAMPLE OF OVERALL COMPOSITION $WO_{2.90}$[a]

Observed values				Calculated values	
d(nm)	I	$\|F\|^2$	$\sin^2\theta \times 10^5$	$\sin^2\theta \times 10^5$	hkl
0.4296	199	131	3,214	3,265	105
0.4019	354	270	3,674	3,675	$\bar{3}01$
0.3904	1,020	827	3,892	3,892	$\bar{3}02$
0.3782	1,571	1,364	4,149	4,152	010
0.3698	1,312	1,195	4,339	4,324	$\bar{3}03$
0.3642	883	831	4,473	4,481	106
0.2837	184	296	7,372	7,417	115
0.2739	1,271	2,213	7,911	7,915, 7,940	403, $\bar{2}08$
0.2716	852	1,511	8,046	8,044	$\bar{3}12$
0.2643	1,013	1,904	8,493	8,476	$\bar{3}13$
0.2623	912	1,742	8,622	8,633	116
0.2541	27	55	9,192		
0.2472	62	134	9,712	9,694	$\bar{2}09$
0.2382	59	138	10,460	10,552	$\bar{2}17$
0.2213	850	2,348	12,110	12,092, 12,067	$\bar{2}18$, 413
0.2148	29	85	12,864		
0.2139	41	121	12,966	13,062	2,010
0.2063	32	102	13,934		
0.1970	236	828	15,288	15,386	2,011
0.1904	789	2,970	16,363	16,324	$\bar{6}05$
0.1890	1,421	5,434	16,617	16,608	020

[a] The sample was shown to contain only {103} *CS* structures by electron microscopy. The most frequently found *n* value was 20, but a significant number of fragments with other *n* values were also seen. X-ray powder data were recorded at room temperature using a Guinier–Hägg camera with strictly monochromatic Cu$K\alpha_1$ radiation. The observed peak intensities I were obtained by a film scanner process and the corresponding $|F|^2$ values after correction for polarization. Lorentz and geometric factors were obtained by computer routines. The calculated $\sin^2\theta$ values were obtained by using a monoclinic cell of a = 1.21 nm, b = 0.378 nm, c = 2.36 nm, and β = 94.6°.

the technique is still subject to this limitation.

The difficulty of X-ray analysis is illustrated in Tables 3 and 4. In these patterns, taken from samples of overall composition $WO_{2.90}$ and $WO_{2.93}$, it is seen that indexing of the films is possible but the uncertainty in this method is high. The problem is that, with the large, low-symmetry unit cells that are found for these phases, high-angle lines can be indexed with a multiplicity of suggestions. Thus, there is little difficulty in finding indices to fit all of the reflections listed in Tables 3 and 4. However, the only way in which the *correct* indices can be derived is by a consideration of the structure factors of the individual reflections. It is then necessary to only use indices which correspond to reflections with reasonably high structure factors. In Table 3 this has been done. The reflections have been indexed in a satisfactory manner as deriving mainly from the oxide $W_{20}O_{58}$, because the structure factor data for $W_{20}O_{58}$ are available in the literature (*1*).

TABLE IV

THE X-RAY POWDER PATTERN OF A SAMPLE OF OVERALL COMPOSITION $WO_{2.93}$[a]

Observed values			
d(nm)	I	$\|F\|^2$	$\sin^2\theta \times 10^5$
0.3969	117	91	3,766
0.3941	156	125	3,820
0.3820	2,860	2,430	4,066
0.3665	2,139	1,986	4,416
0.3120	234	307	6,095
0.3076	163	220	6,270
0.2819	130	212	7,466
0.2741	259	450	7,895
0.2705	1,901	3,400	8,107
0.2644	1,759	3,304	8,486
0.2491	39	83	9,562
0.2208	902	2,493	12,170
0.2144	10	29	12,905
0.2021	60	199	14,521
0.1984	19	65	15,070
0.1953	156	557	15,549
0.1908	1,048	3,927	16,289
0.1877	942	3,652	16,844
0.1830	85	346	17,716
0.1808	130	543	18,156
0.1800	250	1,053	18,301
0.1792	133	565	18,479
0.1739	115	518	19,617
0.1718	20	90	20,090
0.1709	290	1,352	20,319
0.1693	1,195	5,671	20,695
0.1684	1,207	5,784	20,911
0.1656	238	1,177	21,631
0.1560	552	3,036	24,376
0.1550	330	1,834	24,681
0.1539	482	2,713	25,061

[a] Electron microscopy revealed that only {103} *CS* phases were present, with a range of *n* values up to a maximum of 25. The X-ray powder data were recorded and evaluated as in Table III.

The same was not possible for the data in Table 4. Some considerable effort was spent in attempting to index the lines, assuming that the sample was a mixture of phases in the region of $W_{24}O_{70}$ and $W_{25}O_{73}$. There was, of course, little difficulty in assigning indices to each of the lines on the X-ray photograph, but such a procedure is considered as valueless unless other intensity information is available. In Table 4, therefore, we simply record the data, which may be of value to other investigators as they represent typical X-ray data from the $WO_{2.93}$ region of the phase diagram, without further interpretation, but in the knowledge that it represents a mixture of {103} *CS* phases. The problem of indexing and interpreting these complex X-ray photographs will be considered further elsewhere (*29*).

In contrast to this persistent disorder in the *CS* phases, the samples containing only the $W_{24}O_{68}$ structure gave reasonably sharp X-ray diffraction patterns. An example is given in Table 5. Electron microscopy revealed that a certain amount of disorder was still present in these samples in the composition range $WO_{2.82}$–$WO_{2.84}$, but much less than in those heated for shorter periods of time. The X-ray powder pattern seemed of good enough quality to attempt

TABLE V

The X-Ray Powder Pattern of $W_{24}O_{68}$[a]

d_{obsd} (nm)	I_{obsd}	$\lvert F\rvert^2_{obsd}$	$\sin^2\theta_{obsd} \times 10^5$
0.9446	31	3	665
0.8365	63	9	848
0.4187	22	15	3,384
0.4124	18	13	3,488
0.3918	76	60	3,865
0.3834	2,021	1,704	4,037
0.3785	2,539	2,200	4,141
0.3742	49	42	4,238
0.3573	52	50	4,647
0.3481	135	140	4,898
0.3399	62	66	5,137
0.3296	206	240	5,461
0.3242	82	98	5,646
0.3114	136	176	6,118
0.2962	48	70	6,762
0.2795	153	254	7,594
0.2727	320	562	7,980
0.2693	1,635	2,952	8,183
0.2596	91	176	8,805
0.2559	130	262	9,060
0.2483	199	428	9,628
0.2463	60	130	9,779
0.2408	89	204	10,232
0.2399	60	138	10,310
0.2247	107	284	11,757
0.2211	275	756	12,134
0.2195	292	816	12,319
0.2092	180	556	13,556
0.1916	365	1,356	16,161
0.1891	1,161	4,432	16,595
0.1831	140	560	17,701
0.1722	173	794	20,003
0.1708	939	4,382	20,333
0.1696	718	3,396	20,634
0.1652	46	228	21,738
0.1648	134	668	21,845
0.1640	129	648	22,051
0.1615	135	698	22,759
0.1568	289	1,576	24,146
0.1555	822	4,546	24,542
0.1548	195	1,086	24,764

[a] The sample was of overall composition $WO_{2.82}$ heated for 5 months at 1373 K. The data has been recorded in a similar way as described in Table I. The pattern can be indexed using the monoclinic cell parameters $a = 1.931 \pm 2$ nm, $b = 0.3781 \pm 2$ nm, $c = 1.707 \pm 1$ nm, and $\beta = 104.4 \pm 1°$, refined from the cell originally given by Pickering and Tilley (*16*).

to index, as the unit cell is known with a reasonable degree of accuracy (*16*, *18*), and we know that the material is monophasic. However, the problems concerning the correct assignment of indices mentioned above still apply, and it has proved impossible to index high-angle lines categorically in the absence of structure factor or intensity data. The low-angle lines, however, can be indexed with a fair degree of confidence, and this has allowed us to calculate more accurate unit cell parameters than those available from electron diffraction patterns. The improved data for $W_{24}O_{68}$ are

$$a = 1.931 \pm 2 \text{ nm},\ b = 0.3781 \pm 2 \text{ nm},$$
$$c = 1.707 \pm 2 \text{ nm},\ \beta = 104.4 \pm 1°,$$

and the indices of the first seven lines on the film are 200; $\bar{1}02$; $\bar{2}04$; 004; $\bar{3}04$; 104; (010, $\bar{5}03$).

No new phases were found in the samples heated for 5 months, and within this time scale all of the phases reported seemed stable.

Samples Heated at Temperatures of 873 K

The results found for samples heated at temperatures lower than 1373 K are broadly similar to those above. Thus samples prepared at 1273, 1123, 1023, and 873 K still show the same overall pattern of phases in roughly the same composition regions.

The differences that do arise become more pronounced as the temperature of reaction approaches 873 K and it is these results, therefore, we will outline below, which refer to samples heated for 7 weeks. The composition range studied in detail was from WO_3 to $WO_{2.874}$. All the samples were dark blue after reaction and consisted of crystals with a chunky WO_3-like habit similar to the starting material and only a small amount of material with a needle habit.

Superficially the composition range over which {102} *CS* phases occur is much broader in these low-temperature samples, and crystal fragments containing quite well-ordered arrays of {102} *CS* planes with *n* values falling to about 16 have been found, as well as the usual disordered mazes reported above. It is not at all clear if this is a true indication of a real increase in the width of the {102} *CS* phase region, as vapor transport was restricted at 873 K which suppressed the growth of {103} needle crystals. In fact it would seem that these {102} arrays form in crystals of WO_3 by a solid reaction. In either case, it is the only reliable way we have found of preparing reasonably well-ordered arrays of {102} *CS* planes in this system. The contention that the reaction takes place in the WO_3 crystal matrix is supported by the observation that in such crystals disordered *CS* planes are sometimes found which contain regions of {103} *CS* planes as well as {102} *CS* planes. This situation was not found at higher temperatures. The lower composition limit found for these {102} *CS* phases corresponded to $n = 14$, in good agreement with other estimates of this range.

It was found that these {102} *CS* plane arrays were not particularly stable on exposure to the electron beam, and on observation they tended to break up into short segments of {103} *CS* plane type. The resulting crystal microstructures were very disordered. This sort of microstructure was not observed in the high-temperature preparations. Another feature that was observed in these low-temperature preparations that did not occur in the high-temperature preparations is illustrated in Fig. 3. It is seen that large numbers of a new fault are present besides the {102} *CS* planes. These faults are certainly pentagonal columns or groups of pentagonal columns and they were found to occur in large numbers widely distributed throughout the crystals containing *CS* planes, but they appeared to be more prevalent in crystals with rather lower densities of *CS* planes. The fact that the crystals which contain these defects have the same habit as the starting crystals show that these faults have formed by way of a solid-state reaction. Many of the faults were isolated, but others were found at the end of terminating *CS* planes, while others were joined together in chains which were not always straight.

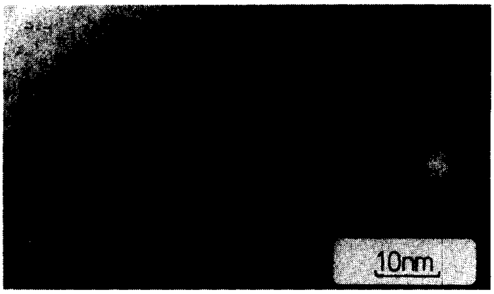

FIG. 3. Electron micrograph of a crystal of WO_3 slightly reduced at 873 K, showing {102} *CS* planes and a fair number of isolated *PC* units. Linked chains of these units also occur in other parts of the crystal.

In addition to the {102} *CS* phases, {103} *CS* structures were also found in these samples. The appearance of crystal fragments containing {103} *CS* plane arrays was very similar to those at higher temperatures and the range of *n* values found was broadly similar to that reported at 1373 K. However, the *CS* planes were rarely so well ordered as at the higher temperatures and consequently the diffraction patterns were more streaked and harder to measure. In the main the well-ordered fragments were presumed to come from needle crystals, but as {103} *CS* planes can also form in bulk crystals (*12*, *19*) this may not be completely true.

The final point to note is that the $W_{24}O_{68}$ phase was not found in any preparations made at 873 K. The phase $W_{18}O_{49}$ was also not present in samples with compositions down to $WO_{2.874}$, but other experiments at 873 K have shown it to form slowly and with its usual whisker-like habit at lower compositions. Such crystals appeared to show no disorder or stoichiometry range, but reaction rates were very sluggish and the latter point was not confirmed by the preparation of monophasic samples.

The Lower Limit of CS Phase Formation

A sample of needle crystals which were {103} *CS* phases and had previously been prepared at 1373 K were heated slowly in air on a thermobalance. At 833 K the specimen started to increase in weight and was completely oxidized when the temperature reached 950 K. These temperatures suggested that the lower limit of *CS* formation would be somewhere below 800 K. In view of the fact that *CS* formation occurred at 873 K, a series of samples were heated at 723 K for 2 months. After this treatment the samples appeared to be unreacted and resembled the starting material both in color and crystal habit. Examination of the samples did not suggest that any incipient reaction had occurred or that an extension of the heating time would change the results. In sealed-tube experiments, therefore, the lower temperature for reaction lies within the temperature range 773 and 873 K.

Discussion

The most general conclusion to be gained from these results is that equilibrium, at least in the strict thermodynamic sense, was not achieved in any of our preparations. The *CS* phases and the $W_{24}O_{68}$ *PC* region were always disordered, even after 5 months heating at 1373 K and at no time did we ever succeed in obtaining a series of two-phase equilibria steps in this structural region. In fact the structures that are formed in the initial reaction do not seem to change a great deal as the heating time is extended. The only exception to this was the WO_2–$W_{18}O_{49}$ region, which behaved classically, as if both phases were strictly stoichiometric.

Before pursuing this point in more detail perhaps it is worth restating that our results apply to the use of sealed-quartz ampoules. This technique may not be the best one for obtaining equilibrium phases, and, moreover, reaction with silicon–oxygen vapor species may also bias the results somewhat. Nevertheless, the quartz ampoule technique has been used almost exclusively by other workers, and as this is the type of result we are trying to correlate, our present data are of value. The shortcomings of the experimental technique should, though, be borne in mind when reading the conclusions presented below.

With this point in mind, we can suggest that although true equilibrium in the thermodynamic sense may not hold, a quasi-equilibrium situation seems to pertain. Thus, if we regard *CS* planes and *PC* elements as defects in a WO_3-like matrix, we do have a strict progression of structure types, and a two-phase structural equilibrium exists. That is, the structures present in the preparations usually fall into only two types, so that we have WO_3 coexisting with WO_3 containing {102} *CS* defects, {102} *CS* coexisting with {103} *CS*, and at lower reductions {103} *CS* coexisting with the $W_{24}O_{68}$ *PC* region. While this description is not of use thermodynamically, it does accurately reflect the rather slow rate of change in these samples and the fact that in practical terms equilibrium holds and that the structural nature of the samples does not vary greatly as heating times are extended. The results of Berglund and Sahle (*19*) fall into a similar pattern. The other points made in the discussion must therefore be viewed in this light and, while equilibrium in a thermodynamic sense might still be distant, equilibrium in a practical sense is quite close to being achieved.

In the regions closest to WO_3, represented by preparations such as $WO_{2.995}$, {102} *CS* planes were always present, and at 873 K, *PC* elements as well. In experimental terms there is no evidence whatsoever to suggest that any oxygen loss is accommodated in terms of classical point defects such as oxygen vacancies. It may seem tautological to suggest that the system is unlikely to expend energy on the formation of these extended defects if point defects are a reasonably accessible alternative, but nonetheless the argument is a valid one. The short *CS* plane nuclei shown in Fig. 2 do not invalidate this argument. Although the darker chevron-like contrast is probably due to elastic strain, surface nucleation of *CS* planes is at least as likely as bulk nucleation. It seems likely, therefore, that in empirical terms, slightly reduced WO_3 contains only {102} *CS* planes, and that reduction leads to the formation of greater and greater densities of these faults, at least for temperatures above about 1000 K.

There is no doubt that continued reduction leads to ordered arrays of {102} *CS* planes and that these seem to form in the matrix of the original WO_3 crystals used as starting material in the experiments. At first sight, though, our results and those of Berglund and Sahle (*19*) are at variance, as they found at 1270 K extensive arrays of {102} *CS* planes, with compositions down to $W_{12}O_{35}$ which, in some cases, coexisted with {103} *CS* plane arrays with compositions of the order of $W_{22}O_{64}$. At this sort of temperature we find only a narrow range for the {102} *CS* phases which coexist with needle-like crystals of {103} *CS* phases of compositions close to $W_{24}O_{70}$. However, at lower temperatures we find microstructures identical to those reported by Berglund and Sahle (*19*).

The difference in these results seems to be associated with the presence or absence of needle-like crystals which form via a vapor pathway. In our experiments these crystals were always present in the preparations made at higher temperatures and lead to the narrow {102} *CS* phase region we found. If this vapor growth is suppressed, as it was in the reactions of Berglund and Sahle, and as it was in our experiments at lower temperatures, then we are dealing with reduction of the bulk WO_3 starting crystals. In this case extensive arrays of {102} *CS* planes form.

Although these two results appear different, they do, in fact, agree perfectly with the theoretical estimates of *CS* plane formation energy put forward earlier (*30–33*) and are explained by considering both the formation energy and relative stability of *CS* planes. It is known that the formation energy of {102} *CS* planes is lower than that of {103} *CS* planes when we consider reduction of WO_3 crystals. Initial reduction of crystals will lead inevitably to the formation of {102} *CS* planes in reduced WO_3 and, provided that no other alternative reaction occurs, will lead to the presence of ordered arrays of {102} *CS* planes, but at the expense of a considerable increase in the elastic strain energy of the crystals. This elastic strain energy is sufficient to make ordered arrays of {103} *CS* planes preferred over ordered arrays of {102} *CS* planes. This result is confirmed by observations on the transformation of {102} *CS* to {103} *CS* planes, where even the rather modest temperatures experienced by crystal flakes during electron microscope observation cause {102} *CS* arrays to transform, as far as possible, to {103} arrays, but never vice versa. At a degree of reduction corresponding to somewhere in the region of $W_{12}O_{35}$–$W_{16}O_{27}$, the elastic strain energy is unreasonably large, and the crystals can become more stable by changing to a {103} array. This, however, is rather a difficult solid-state process.

If a vapor pathway is available the higher formation energy of {103} *CS* planes in a WO_3 matrix becomes irrelevant. At this stage the lower elastic strain energy and hence free energy of the {103} materials dominates, and so they form in preference. It seems reasonable to suggest, therefore, that sealed-tube experiments with a vapor pathway available produce products which are nearer to true equilibrium.

The gradual increase in the $W_{24}O_{68}$ phase structure as heating times increase suggests that it may form, in our experiments, from a {103} *CS* phase precursor. This is supported indirectly by the observation that crystal fragments were found which contain elements of both the $W_{24}O_{68}$ structure and {103} *CS* planes. It does not automatically follow, though, that we have evidence of a sequential reduction reaction as a similar result would be anticipated simply by a change in overall stoichiometry of the fragment from one region to another. A series of experiments to investigate this further would be of interest and is planned for the future.

Because of the structural nature of the disorder in the $W_{24}O_{68}$ crystals it has always seemed reasonable to suppose that a series of such phases would occur characterized by sheets of rotation faults separated by slabs of WO_3-like structure (*18, 22*). To date in our studies we have not found any evidence for such a series, but other compounds may occur under different preparative conditions than those employed here, and as heating times of up to 5 months were used, it now seems likely that different preparation methods will have to be used or else such phases may need to be stabilized by the addition of other atomic species.

Finally we turn to the question of the microstructures found in the disordered phases. In the past analysis has shown that elastic strain energy has played an important part in controlling the microstructures of the *CS* phases (*30–33*). The present results tend to support this contention. If we look at Table 2 we find that in the oxygen-rich end of the phase region, the oxide $W_{24}O_{70}$ forms in preference to the neighboring phases and at the metal-rich end of the phase region the oxide $W_{18}O_{52}$ is the commonest one found. Both of these are particularly stable phases (*30*), showing that despite the fact that equilibrium has not been achieved in the strict sense, the distribution of phases is in quite good accord with the expectations of strain energy calculations.

A similar consideration applies to the *PC* phases. It has been suggested that the *PC* unit produces a lower degree of elastic strain energy in the WO_3 matrix than the *CS* plane unit (*22*). This has been taken to imply that *PC* phases would be favored at lower temperatures or higher degrees of reduction than *CS* phases. The trend is followed here. In the region near to WO_3, *PC* elements were found in samples heated at 873 K. If the crystals could be reduced at lower temperatures, perhaps employing hydrothermal techniques, a phase of the $W_{24}O_{68}$ type may well form at low degrees of reduction and may lead to the formation of the phases related to $W_{24}O_{68}$ referred to above. The existence of *PC* elements at the end of *CS* planes, illustrated by Sahle and Sundberg (*20*), also reflects the role of *PC* elements in reducing elastic strain. At the end of a *CS* plane we have a region of high elastic strain, associated with a collapse of the crystal structure. The existence of *PC* elements allows this strain field to be dissipated.

In conclusion we can say that equilibrium in the W–O system within the composition range WO_3 to approximately $WO_{2.80}$ is difficult to achieve using ordinary sealed-tube preparative techniques. In order to prepare any of the compounds pure it is likely that very careful control of temperature and ambient oxygen pressure is necessary. Despite the large number of studies so far carried out, there is still the possibility that new *PC* phases can form in the system at low temperatures if the kinetic barriers to reaction can be overcome.

Acknowledgments

T.E. is grateful to Professor Arne Magnéli for the experimental facilities put at his disposal and to the

Swedish Natural Science Research Council, which sponsored part of these studies. E.I. is indebted to Professor R. Wada for his encouragement during this work. We are also indebted to Professor L. Kihlborg and Margareta Sundberg for helpful discussions.

References

1. A. Magnéli, *Ark. Kemi* **1,** 513 (1950).
2. A. Magnéli, *Ark. Kemi* **1,** 223 (1949).
3. A. Magnéli, *Ark. Kem Mineral. Geol. A* **24,** No. 2 (1946).
4. P. Gadó and A. Magnéli, *Acta Chem. Scand.* **19,** 1514 (1965).
5. E. Gebert and R. J. Ackermann, *Inorg. Chem.* **5,** 136 (1966).
6. G. R. St. Pierre, T. W. Ebihara, M. J. Pool, and R. Speiser, *Trans. AIME* **224,** 259 (1962).
7. B. Phillips and L. L. Y. Chang, *Trans. AIME* **230,** 1203 (1964).
8. L. L. Y. Chang and B. Phillips, *J. Amer. Ceram. Soc.* **52,** 527 (1969).
9. R. J. D. Tilley, *Mater. Res. Bull.* **5,** 813 (1970).
10. J. G. Allpress, R. J. D. Tilley, and M. J. Sienko, *J. Solid State Chem.* **3,** 440 (1971).
11. S. Iijima, *J. Solid State Chem.* **14,** 52 (1974).
12. M. Sundberg and R. J. D. Tilley, *J. Solid State Chem.* **11,** 150 (1974).
13. J. G. Allpress and P. Gadó, *Cryst. Lattice Defects* **1,** 331 (1970).
14. M. Sundberg, *J. Solid State Chem.* **35,** 120 (1980).
15. M. Sundberg, *Acta Crystallogr. Sect. B* **32,** 2144 (1976).
16. R. Pickering and R. J. D. Tilley, *J. Solid State Chem.* **16,** 247 (1976).
17. O. Glemser, J. Weidelt, and F. Freund, *Z. Anorg. Allg. Chem.* **332,** 299 (1964).
18. M. Sundberg, *Chem. Scr.* **14,** 161 (1978–1979).
19. S. Berglund and W. Sahle, *J. Solid State Chem.* **36,** 66 (1981).
20. W. Sahle and M. Sundberg, *Chem. Scr.* **16,** 163 (1980).
21. R. J. D. Tilley, *Chem. Scr.* **14,** 147 (1978–1979).
22. T. Ekström and R. J. D. Tilley, *Chem. Scr.* **16,** 1 (1980).
23. V. K. Sarin, *J. Mater. Sci.* **10,** 593 (1975).
24. B. G. Brandt and A. G. Nord, *Chem. Commun. Univ. Stockholm* No. 5 (1970).
25. E. Iguchi, *J. Phys. Chem. Solids* **38,** 1039 (1977).
26. T. Ekström and R. J. D. Tilley, *J. Solid State Chem.* **16,** 141 (1976).
27. J. E. Marucco, P. Gerdanian, and M. Dode, *J. Chim. Phys.* **66,** 674 (1969).
28. T. Ekström, *Chem. Commun. Univ. Stockholm* No. 7 (1975).
29. M. Sundberg, T. Ekström, and R. J. D. Tilley, in preparation.
30. E. Iguchi and R. J. D. Tilley, *Philos. Trans. Roy. Soc. London A* **286,** 55 (1977).
31. E. Iguchi and R. J. D. Tilley, *J. Solid State Chem.* **24,** 121 (1978).
32. E. Iguchi and R. J. D. Tilley, *J. Solid State Chem.* **24,** 131 (1978).
33. E. Iguchi and R. J. D. Tilley, *J. Solid State Chem.* **32,** 221 (1980).